Cancer Chemother Pharmacol (2005) 55: 79–90
DOI 10.1007/s00280-004-0849-3

ORIGINAL ARTICLE

Ming-Jie Liu · Zhao Wang · Yong Ju
Ricky Ngok-Shun Wong · Qing-Yu Wu

Diosgenin induces cell cycle arrest and apoptosis in human leukemia K562 cells with the disruption of Ca^{2+} homeostasis

Received: 28 January 2004 / Accepted: 22 April 2004 / Published online: 14 September 2004

Abstract *Purpose*: Diosgenin is a steroidal sapogenin with estrogenic and antitumor properties. In order to elucidate the mechanism of its antiproliferative activity, we investigated its effects on the cell cycle and apoptosis in human chronic myelogenous leukemia K562 cells. *Methods*: Cell viability was assessed via an MTT assay. Apoptosis was investigated in terms of nuclear morphology, DNA fragmentation, and phosphatidylserine externalization. Cell cycle analysis was performed via PI staining and flow cytometry (FCM). Western blotting and immunofluorescence methods were used to determine the levels of p53, cell cycle-related proteins and Bcl-2 family members. FCM was also used to estimate the changes in mitochondrial membrane potential (MMP), intracellular Ca^{2+} concentration and reactive oxygen species (ROS) generation. *Results*: Cell cycle analysis showed that diosgenin caused G_2/M arrest independently of p53. The levels of cyclin B1 and $p21^{Cip1/Waf1}$ were decreased, whereas cdc2 levels were increased. Subsequent apoptosis was demonstrated with the dramatic activation of caspase-3. A dramatic decline in intracellular Ca^{2+} concentration was observed as an initiating event in the process of cell cycle arrest and apoptosis, which was followed by the hyperpolarization and depolarization of MMP. Generation of ROS was observed in the progression of apoptosis. The antiapoptotic Bcl-2 and Bcl-x_L proteins were downregulated, whereas the proapoptotic Bax was upregulated. *Conclusions*: Diosgenin inhibits K562 cell proliferation via cell cycle G_2/M arrest and apoptosis, with disruption of Ca^{2+} homeostasis and mitochondrial dysfunction playing vital roles.

Keywords Diosgenin · Apoptosis · Cell cycle arrest · Ca^{2+} homeostasis · Mitochondrial hyperpolarization

M.-J. Liu · Z. Wang (✉) · Q.-Y. Wu (✉)
Department of Biological Sciences and Biotechnology,
Tsinghua University, Beijing, People's Republic of China
E-mail: zwang@tsinghua.edu.cn
Tel.: +86-10-62772241
Fax: +86-10-62772240
Tel.: +86-10-62772241
Fax: +86-10-62772240

Z. Wang
Institute of Biomedicine,
Tsinghua University, Beijing,
People's Republic of China

Y. Ju
Key Laboratory of Bioorganic Phosphorus Chemistry,
Department of Chemistry, Tsinghua University,
Beijing, People's Republic of China

R. N.-S. Wong
Department of Biology, Hong Kong Baptist University,
Hong Kong, People's Republic of China

Introduction

Diosgenin is a steroidal sapogenin belonging to the group of triterpenes (Fig. 1). It is found in several plants including Dioscorea species (yams), fenugreek and *Costus speciosus*. Steroidal sapogenins are secondary metabolites whose biosynthetic precursors are sterols, especially cholesterol. They are mainly found as glycosides called steroidal saponins, which constitute a structurally diverse class of natural products and are one of the major components in traditional Chinese medicines [3]. Diosgenin is a very important compound in the pharmaceutical industry as a natural source of steroidal hormones. Recent studies have found that it can be absorbed through gut and plays an important role in the control of cholesterol metabolism [29]. Other investigators have reported that it has estrogenic effects [1] and antitumor activities [5, 15, 25]. As a new megakaryocytic differentiation inducer [4], diosgenin could cause changes in lipoxygenase activities in human erythroleukemia cells [26]. It induces p53-mediated cell cycle G_1 arrest and apoptosis in osteosarcoma cells, and its proapoptotic activity is greater than that of two other plant steroids, hecogenin and tigogenin [5, 25].

It is necessary to study the biochemical and cellular mode of action of this attractive natural product,

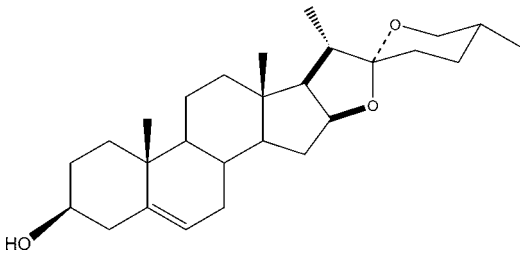

Fig. 1 Chemical structure of diosgenin

particularly on targets against which it may be used as a pharmaceutical agent. Treatment of tumor cells with cytotoxic agents usually results in the breakdown of the cell cycle machinery, the cells subsequently entering into programmed cell death or apoptosis. Cell cycle checkpoints establish the timing and strength of arrest, repair and apoptotic responses to a damaging agent [11]. Molecules regulating cell division, such as cyclin-dependent kinases (CDKs) and inhibitors for CDKs, are also implicated in regulating apoptosis. The G_2/M transition is regulated by cdc2 kinase and cyclin B1 which are maturation-promoting factors that determine entry into mitosis [2]. The tumor suppressor p53 and its downstream transcriptional target $p21^{Cip1/Waf1}$ are also essential to sustain G_2/M phase arrest after DNA damage through the inhibition of cdc2 [30]. In addition, recent studies suggest that caspase-mediated cleavage of $p21^{Cip1/Waf1}$ is a critical step in converting cancer cells from growth arrest to apoptosis [34].

Apoptosis has been described as a highly regulated process, in which caspases are involved in both commitment and execution phases, resulting in the cleavage of specific substrate proteins [31]. Mitochondria play the pivotal roles that integrate diverse apoptotic stimuli into a core intrinsic death pathway [13]. The control of apoptosis is governed by the Bcl-2 family proteins, which include antiapoptotic Bcl-2 and Bcl-x_L and proapoptotic Bax and Bak; the balance between these opposing activities is regulated by a third subgroup called the "BH_3-only" proteins [6]. Apoptosis induced by extracellular cues and internal insults such as DNA damage occurs mainly through the mitochondria-dependent pathway, with perturbation of the mitochondrial inner membrane as an early event. It is caused by the opening of the permeability transition pore (PTP) complex, resulting in the decline of mitochondrial membrane potential (MMP, $\Delta\Psi_m$). The apoptotic stress causes Bax to translocate from cytosol to mitochondria, leading to an efflux of proapoptotic proteins that normally reside in the intermembrane space, such as cytochrome *c* [8] and AIF. Cytochrome *c* then complexes with Apaf-1 and caspase-9 to form an apoptosome, which activates the effector caspases including caspase-3, resulting in the disassembly of the cell [17].

Disruption of intracellular Ca^{2+} homeostasis has been proposed as a critical event in the initiation of apoptosis, which results from various effects on Ca^{2+} compartmentalization processes [7]. Mitochondrial Ca^{2+} uptake may serve as a regulatory mechanism to modulate Ca^{2+} signaling and oxidative phosphorylation [10]. The overloading of Ca^{2+} has detrimental effects, both in terms of an enhanced production of reactive oxygen species (ROS) and by the fact that mitochondrial Ca^{2+}-cycling may result in mitochondrial depolarization through the opening of the PTP, finally culminating in mitochondrial dysfunction and apoptosis.

Defective cell cycling and apoptotic mechanisms are considered to play a role in both the development of malignancy and resistance to chemotherapeutic drugs [18]. A better understanding of the essential biochemical events involved in cytotoxic stress-induced apoptosis is important for developing rational chemotherapeutic approaches. In this study, we investigated the effects of diosgenin on cell cycle progression and apoptosis in human chronic myelogenous leukemia (CML) K562 cells. The results demonstrated that diosgenin can inhibit proliferation via blocking cell cycle progression at the G_2/M phase and subsequently progression to apoptosis. The underlying events relevant to mitochondria were studied in detail, including the alteration of MMP, the generation of ROS and failure of control of Ca^{2+} homeostasis. The regulation of Bcl-2 family members was also investigated.

Materials and methods

Cell culture

The human CML cell line K562 was kindly provided by Dr. Li-Sheng Wang (Academy of Military Medical Sciences, Beijing). Human promyelocytic leukemia NB_4 cells were kindly provided by Dr. Zhu Chen (Rui-jin Hospital, Shanghai Institute of Hematology, Shanghai Second Medical University). Cells of both cell lines were cultured in RPMI 1640 medium (GIBCO BRL, Life Technologies, Invitrogen Corporation, Carlsbad, Calif.), with 10% fetal bovine serum (FBS) (Hyclone Laboratories, Logan, Utah), 100 IU/ml penicillin, and 100 μg/ml streptomycin in humidified air at 37°C with 5% CO_2.

Materials

Diosgenin was purchased from Sigma Chemical Co. (St Louis, Mo.). It was dissolved in ethanol (100 μ*M*) and mixed with the fresh medium to achieve the desired concentration. The final ethanol concentration in all cultures was 0.5%, which did not alter cell growth and cell cycle measurements when compared with the vehicle-free medium. Wright–Giemsa stain (modified), propidium iodide (PI), 3-(4,5-dimethyl-thiazol-2-yl)-2,5-diphenyl-tetrazolium bromide (MTT), saponin, etoposide and mouse anti-*β*-actin monoclonal antibody (clone AC-74) were also bought from Sigma. 4′,6-Diamidin-2′-phenylindol-dihydrochloride (DAPI) was purchased from Roche Diagnostics (Mannheim, Germany).

2′,7′-Dichlorodihydrofluorescein diacetate (DCFH-DA), 3′,3′-dihexyloxacarbocyanine ($DiOC_6(3)$) and Fluo-3 were purchased from Fluka Chemie (Sigma-Aldrich, Steinheim, Switzerland). Rabbit anti-Bax polyclonal antibody (clone N-20), mouse anti-Bcl-x_L monoclonal antibody (clone H-5), mouse anti-p21 monoclonal antibody (clone 187), mouse anti-cdc2 monoclonal antibody (clone 17), and mouse anti-cyclin B1 monoclonal antibody (clone GNS1) were all purchased from Santa Cruz Biotechnology (Santa Cruz, Calif.).

Cell viability

K562 cells were suspended at a final concentration of 5×10^4 cells/ml and seeded in 96-well microtiter plates. Various concentrations (6.25–66.7 μ*M*) of diosgenin were added to each well in triplicate. After incubation for the indicated times, the viable cells were counted by the trypan blue exclusion method. The inhibitory effects were also determined by the MTT assay. After exposure to diosgenin, cells were incubated with MTT (0.5 mg/ml) for 4 h. The formazan precipitate was dissolved in 200 μl dimethyl sulfoxide and the absorbance at 550 nm was measured with a Benchmark microplate reader (Bio-Rad, Hercules, Calif.).

Cytomorphology

The cells were directly observed under an inverted phase-contrast microscope (Leica DMIRB) and recorded using a Leica CCD camera (DC200) (Leica Microsystems Wetzlar, Germany). The nuclei in the same visual field were stained with DAPI (10 μg/ml) and recorded by fluorescence microscopy (Leica DMIRB and MPS60). Meanwhile, the cells were centrifuged onto slides by a cytospin (700 rpm, 5 min), stained with Wright–Giemsa dye, and examined under a microscope (Leica DMLB and MPS60).

Flow cytometric analysis of cell cycle and apoptosis

Cells were fixed by 70% ethanol at −20°C for at least 12 h. After two washes with phosphate-buffered solution (PBS), the cells were incubated in RNase A/PBS (100 μg/ml) at 37°C for 30 min. Intracellular DNA was labeled with PI (50 μg/ml) and analyzed with a FACSCalibur fluorescence-activated cell sorter (FACS) using CELLQuest software (Becton Dickinson, NJ). The cell cycle profile was obtained by analyzing 15,000 cells using the ModFIT LT 3.0 program (Becton Dickinson). Surface exposure of phosphatidylserine on apoptotic cells was measured using an ApoAlert Annexin V-FITC apoptosis detection kit (BD Biosciences Clontech, CA). Cells were treated according to the manufacturer's instructions and determined with a Coulter EPICS Elite flow cytometer (Coulter Corporation). Additional exposure to PI made it possible to differentiate early apoptotic cells (annexin-positive and PI-negative) from late apoptotic cells (annexin-positive and PI-positive).

DNA fragmentation assay

The untreated and diosgenin-treated cells were harvested and lysed in 100 μl buffer (10 m*M* Tris-HCl, pH 7.4, 10 m*M* EDTA, pH 8.0, 0.5% Triton X-100). The supernatant obtained following centrifugation at 14,000 *g* for 10 min was incubated with RNase A (200 μg/ml) at 37°C for 60 min. Proteins were removed by incubation with Proteinase K (200 μg/ml) at 50°C for 30 min. To the lysate was added 20 μl 5 *M* NaCl and 120 μl isopropanol. After 12 h at −20°C, the precipitated DNA pellet was dissolved in Tris-acetate-EDTA buffer, electrophoresed in a 1.5% agarose gel, stained with ethidium bromide, and photographed under UV illumination.

Assessment of caspase activity

The upstream sequence of the specific site recognized by active caspase-3 is DEVD (Asp-Glu-Val-Asp). For detection of caspase-3 activation, an ApoAlert caspase fluorescent assay kit (BD Biosciences Clontech, Calif.) was used, which is based on the fluorescence spectrophotometric detection of 7-amino-4-trifluoromethyl coumarin (AFC) after cleavage from the substrate DEVD-AFC in the presence of cytosolic extracts. Treated and control cells were resuspended in cell lysis buffer and incubated on ice for 10 min. After centrifugation, equal amounts of protein from cytosolic extracts (150 μg) were diluted in reaction buffer containing dithiothreitol (DTT) and incubated with DEVD-AFC (200 μ*M* final concentration) at 37°C for 2 h. The AFC fluorescence absorbance was then quantified in a spectrophotometer (Hitachi F-2500, Japan). Background readings from cell lysates and buffers were subtracted from the reading for each sample. At least three independent experiments were performed using separate cultures.

Analysis of intracellular Ca^{2+} concentration

Changes in intracellular Ca^{2+} concentration were determined by a fluorescent dye, Fluo-3. Cells were washed twice with RPMI 1640 media and incubated with 5 μ*M* Fluo-3 at 37°C for 30 min. Then the cells were washed and subjected to FACS analysis.

Measurement of mitochondrial membrane potential

Mitochondrial energization was determined by the retention of the dye $DiOC_6(3)$. About 1 million cells

were harvested and washed twice with PBS. After incubation with 50 nM $DiOC_6(3)$ at 37°C for 30 min, the cells were washed again and analyzed with FACS.

Measurement of intracellular ROS

Intracellular ROS production was measured using a fluorescent dye, DCFH-DA, which is converted to DCFH by esterases when the cell takes it up. DCFH is reactive with ROS to give a new highly fluorescent compound, dichlorofluorescein, which can be analyzed with FACS. The treated cells were incubated with DCFH-DA (10 μ*M*) at 37°C for 1 h, and then measured with the FACS.

Immunofluorescence analysis

Cells were harvested and washed twice with PBS containing 3% FBS. After fixing in 4% paraformaldehyde at 4°C for 15 min, cells were washed and resuspended in PBS buffer containing 0.2% saponin and 5% FBS. The FITC-conjugated mouse anti-human Bcl-2 and p53 monoclonal antibodies and their IgG_1 isotype-matched control (BD Biosciences PharMingen, Calif.) were added. After incubation at 4°C for 30 min, the cells were washed and subjected to FACS analysis.

Western blotting

Cells were harvested and washed with PBS. The lysates were obtained using lysis buffer (150 m*M* NaCl, 10 m*M* Tris, pH 7.4, 5 m*M* EDTA, pH 8.0, 1% Triton X-100, 1 m*M* PMSF, 20 μg/ml aprotinin, 50 μg/ml leupeptin, 1 m*M* benzidine, 1 μg/ml pepstatin), followed by centrifugation (10,000 *g*, 20 min). Total protein concentration in the supernatant was determined using a bicinchoninic acid assay (Beyotime Biotechnology, China). Proteins were normalized to 50 μg per lane, resolved on 12.5% polyacrylamide gels, and subsequently blotted onto PVDF membranes. After blocking with TTBS (100 m*M* Tris-HCl, pH 7.5, 0.9% NaCl, 0.1% Tween 20) containing 5% (w/v) skimmed milk, the membranes were incubated with primary and secondary antibodies at room temperature. Then, the membranes were washed with TTBS and detected using an ECF western blotting kit. The densities of sample bands were determined with a Storm 860 fluorescence scanner and analyzed with ImageQuant software (Amersham Biosciences).

Statistical analysis

One-way analysis of variance (ANOVA) was performed to determine the significance of differences between groups. *P* values less than 0.05 were considered statistically significant.

Results

Diosgenin suppresses the growth of K562 cells

Cell proliferation was evaluated daily based on the ability of the cells to exclude trypan blue. Diosgenin induced a marked time-dependent and dose-dependent diminution of cell viability as early as 24 h, indicating that the proliferation potential of the cells was impaired (Fig. 2a). The IC_{50} (median growth-inhibitory concentration) determined by the MTT assay, was about 15 μ*M* (Fig. 2b).

Diosgenin induces cell cycle G_2/M arrest and apoptosis in K562 cells

Figure 3 shows representative morphological changes of K562 cells when exposed to diosgenin (20 μ*M*) for 48 h.

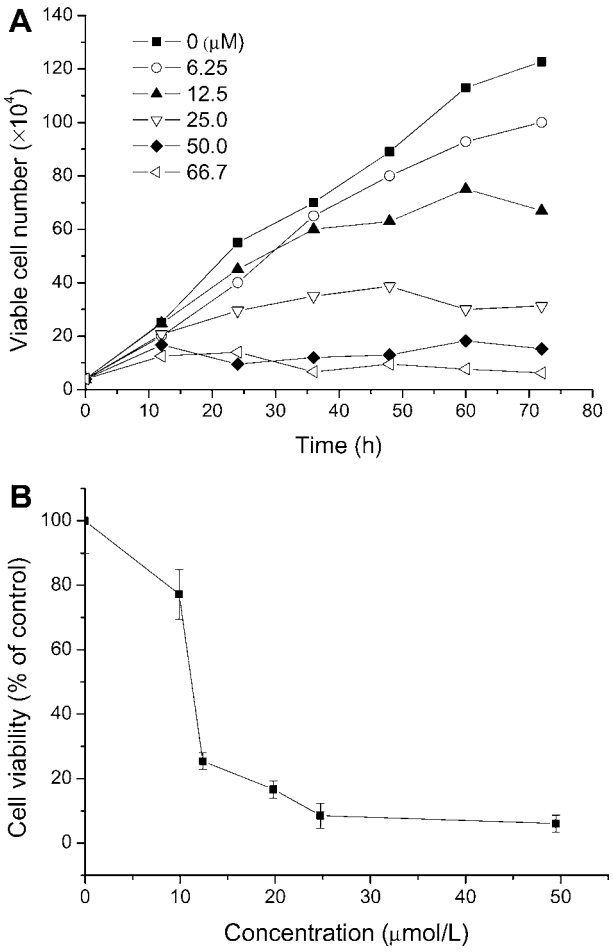

Fig. 2a, b Effects of diosgenin on the proliferation and viability of K562 cells. **a** 562 Cells were incubated with different concentrations of diosgenin for the indicated times. The number of viable cells was measured in triplicate by the trypan blue exclusion assay. Each point represents the mean of the data from three independent experiments. **b** K562 cells were treated with diosgenin at the indicated concentrations for 72 h. The viability was determined by the MTT assay. Each point is the mean of three replicates; *bars* represent the standard deviation

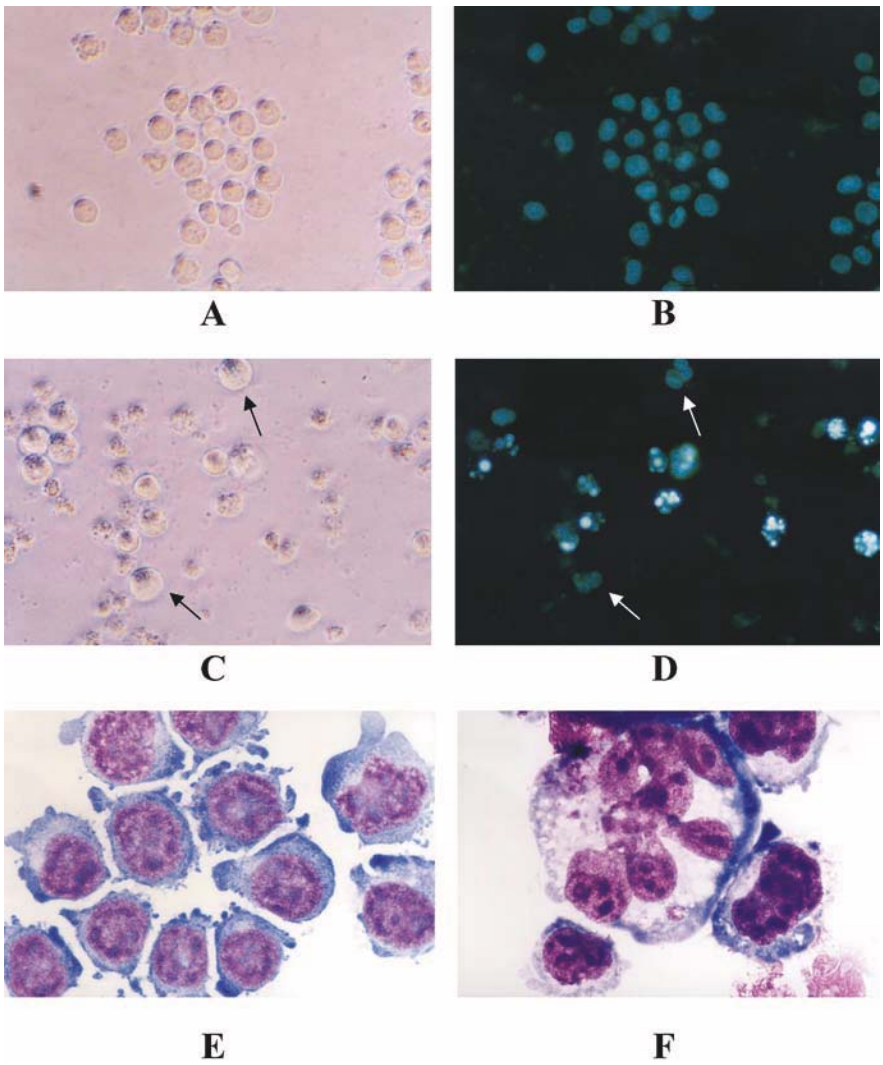

Fig. 3a–f Morphological changes of K562 cells after exposure to diosgenin (20 μ*M*) for 48 h. **a**, **c** Phase-contrast microscopic view; **b**, **d** fluorescence microscopic view of the same visual field as **a**, **c**; (**a**, **b** untreated cells; **c**, **d** cells treated with diosgenin). Condensed chromosomes are seen as spots in the nucleus by DAPI staining (*arrows* multinuclear cells; ×400). **e**, **f** Wright–Giemsa staining of untreated and diosgenin-treated cells (×1000)

Under control conditions, K562 cells appeared normal and the nuclei were round and homogeneous (Fig. 3a, b, e). After treatment with diosgenin, the cells exhibited the characteristic features of apoptosis, with nuclear condensation and fragmentation as indicated by DAPI staining (Fig. 3d). In addition, the treated cells showed a marked increase in cellular size (Fig. 3c, d, arrows), cytoplasmic content and nuclear complexity, which was also seen in the slides stained by Wright–Giemsa dye (Fig. 3f). In order to determine whether the cells had undergone differentiation towards megakaryocyte, the expression of CD41 was determined using PMA as a positive control. The results indicated that diosgenin cannot be used as an inducer (data not shown). Then the cell cycle distributions were determined at the indicated times. At a concentration of 20 μ*M* for 36 h, diosgenin induced a significant increase in cell population in the G_2/M phase (Fig. 4a). Since cyclin B1-cdc2 is known to be critical for the G_2-M transition, their expression levels were determined by Western blot analysis (Fig. 4b). Compared with the control, the levels of cyclin B1 decreased in a time-dependent manner, coinciding with the effective mitotic-arresting process. One the other hand, the cdc2 levels increased in response to diosgenin but then remained at a steady level. It is interesting that $p21^{Cip1/Waf1}$, an inhibitor of CDKs, was downregulated in time-dependent manner. We speculate that $p21^{Cip1/Waf1}$ may be cleaved during the apoptotic process, although we did not detect the cleaved fragments. Since K562 cells lack functional p53, we performed similar experiments on p53-expressing human promyelocytic leukemia NB_4 cells in order to assess the possible role of p53. NB_4 cells treated with diosgenin increased in size and cell cycle G_2/M arrest, and polyploid cells appeared (Fig. 5a, b). Of special interest is that diosgenin increased the p53 levels in NB_4 cells, indicating its role in the control of cell cycle G_2/M arrest (Fig. 5c).

Flow cytometric sub-G_1 analysis showed that a dramatic hypodiploid population of K562 cells appeared following treatment with diosgenin for 48 h (Figs. 4a, 6a), together with DNA fragmentation (Fig. 6b). Furthermore, the annexin V/PI binding assay was performed to detect the redistribution of phosphatidylserine, which is a marker of early apoptotic cells (Fig. 6c).

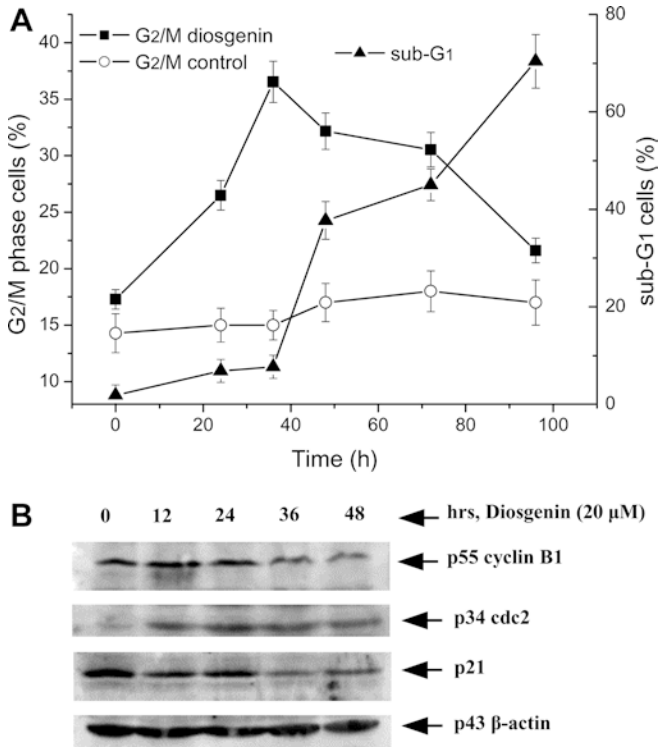

Fig. 4a, b Effects of diosgenin on cell cycle distribution and mitosis-related proteins in K562 cells. **a** K562 cells were treated with diosgenin (20 μM) for the indicated times. The percentages of G_2/M and sub-G_1 cells were evaluated by PI staining and flow cytometric analysis. **b** Western blot analysis of cdc2, cyclin B1 and $p21^{Cip1/Waf1}$ levels in lysates from untreated and diosgenin-treated K562 cells. β-actin was used as an internal control to normalize the amounts of proteins loaded in each lane

In untreated K562 cells, 3.8% of cells were annexin V-positive/PI-negative, whereas 4.3% of cells were annexin V/PI double positive. After treatment with 20 μM diosgenin for 48 h, the annexin V-positive/PI-negative cells increased to 20.1% and the double-positive cells increased to 55.6%. Furthermore, from 72 to 96 h, there was a decrease in G_2/M blockade and a reciprocal increase in the sub-G_1 population (Fig. 4a), suggesting that K562 cells were arrested followed by apoptotic cell death. The G_1 and S phases in the surviving fraction became clearer after cells in the G_2/M phase had been removed by apoptosis.

Diosgenin induces a dramatic decline in intracellular Ca^{2+} concentration

Treatment with diosgenin rapidly reduced the intracellular Ca^{2+} levels, with the effect being apparent by as early as 5 h (Fig. 7). The intensity of Fluo-3 fluorescence reached a minimum at 9 h and increased after that, indicating that the decline in intracellular Ca^{2+} concentration was an important initial step for diosgenin-induced cell cycle arrest and apoptosis. It should be pointed out that a later increase in Ca^{2+} concentration was essential for the progression of apoptosis.

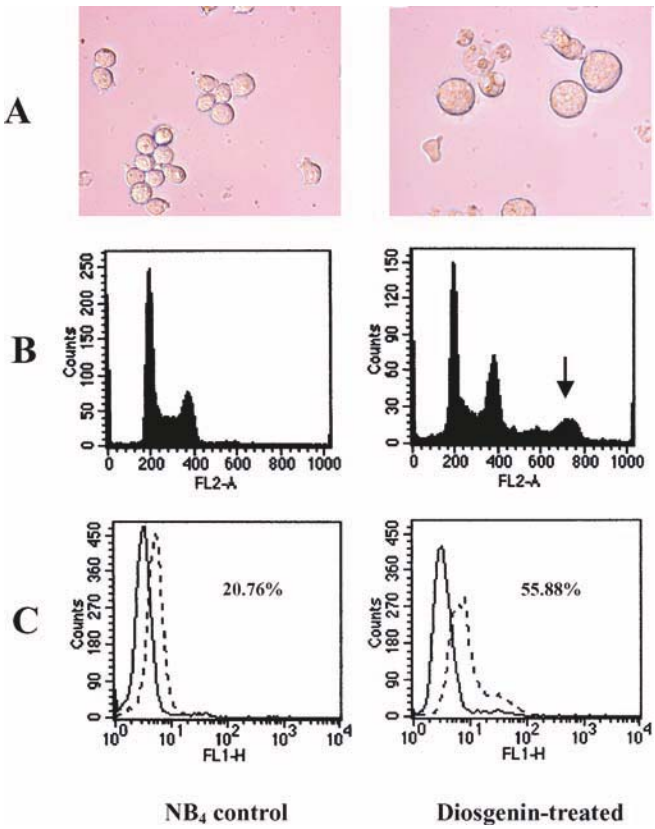

Fig. 5a–c Effects of diosgenin on human leukemia NB_4 cells. **a** Morphological changes in NB_4 cells treated with 10 μM diosgenin for 48 h. Phase-contrast microscopic images were acquired using Leica CCD camera (DC200). **a** Cell cycle G_2/M arrest and the appearance of polyploid cells (*arrow*) in NB_4 cells treated with 10 μM diosgenin for 24 h. **a** Immunofluorescence analysis of p53 expression in NB_4 cells exposed to 10 μM diosgenin for 24 h. The *solid lines* indicate mouse $IgG_{1\kappa}$ used as isotype control while the *dotted lines* represent diosgenin-treated NB_4 cells

Diosgenin induces biphasic alterations in MMP, with mitochondrial hyperpolarization as a primary response

When $\Delta\Psi_m$ of K562 cells was estimated using the probe $DiOC_6(3)$, a significant hyperpolarization of mitochondria occurred after 24 h of treatment, rather than a primary decrease in $\Delta\Psi_m$, which was typical of apoptosis (Fig. 8). At 48 h, the hyperpolarization peak decreased and the depolarization peak, corresponding to a much lower fluorescence, increased, indicating the collapse of the inner mitochondrial membrane. Dissipation of $\Delta\Psi_m$ might be have been caused by opening of the mitochondrial PTP.

Diosgenin induces activation of caspase-3 and generation of ROS

We then sought to determine whether caspases were involved in the cell death response induced by diosgenin. As shown in Fig. 9a, diosgenin (20 μM) induced a dramatic and sustained increase in caspase-3 activity in

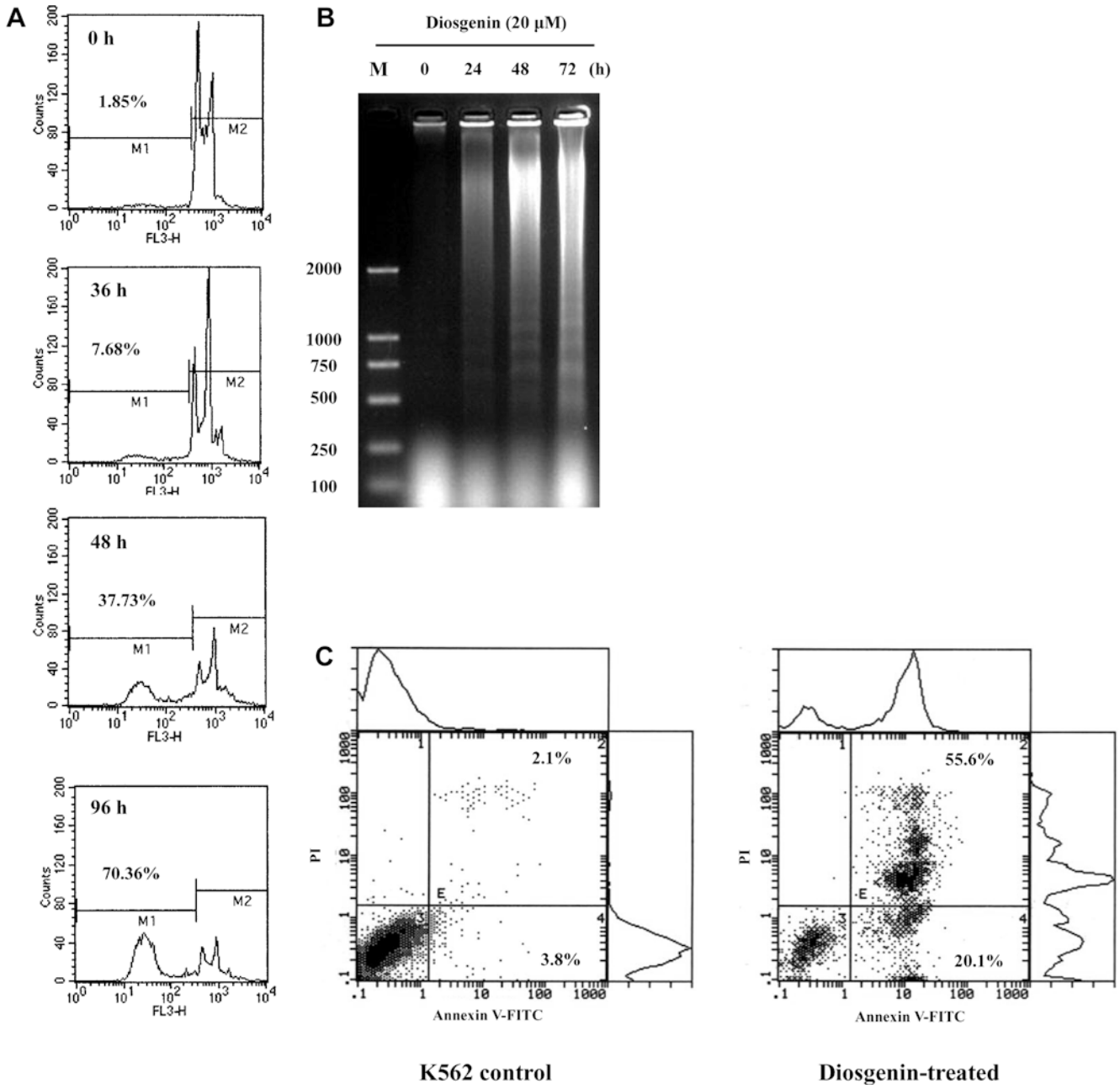

Fig. 6a, b Diosgenin induces apoptosis of K562 cells in a time-dependent manner. **a** K562 cells were treated with 20 μ*M* diosgenin for the indicated times. Apoptosis was evaluated in terms of the proportion of cells in the sub-G_1 phase by flow cytometric analysis. **b** Induction of internucleosomal DNA fragmentation in response to diosgenin exposure for the indicated times. **c** Flow cytometric analysis of phosphatidylserine externalization (annexin V binding) and cell membrane integrity (PI staining). K562 cells were treated with diosgenin (20 μ*M*) for 48 h. The dual parametric dot plots combining annexin V-FITC and PI fluorescence show the viable cell population (*lower left quadrant*, annexin V^- PI^-), the early apoptotic cells (*lower right quadrant*, annexin V^+ PI^-), and the late apoptotic cells (*upper right quadrant*, annexin V^+ PI^+)

K562 cells. After 48 h of treatment, the enzyme activity was approximately 13-fold higher than that of the control group, demonstrating that activation of the effector caspase was responsible for apoptosis induced by diosgenin. On the other hand, the generation of ROS was determined by DCFH-DA fluorescence. When K562 cells were treated with 20 μ*M* diosgenin, the fluorescent intensity increased gradually in a time-dependent manner (Fig. 9b), suggesting that continuous generation of ROS is involved in the apoptotic process.

Involvement of Bcl-2 family members in diosgenin-induced apoptosis

Experiments were performed to estimate intracellular levels of Bcl-2 family members in diosgenin-treated cells. Figure. 10a shows the representative immunofluorescence results of Bcl-2. The immunofluorescence decreased gradually in a time-dependent manner.

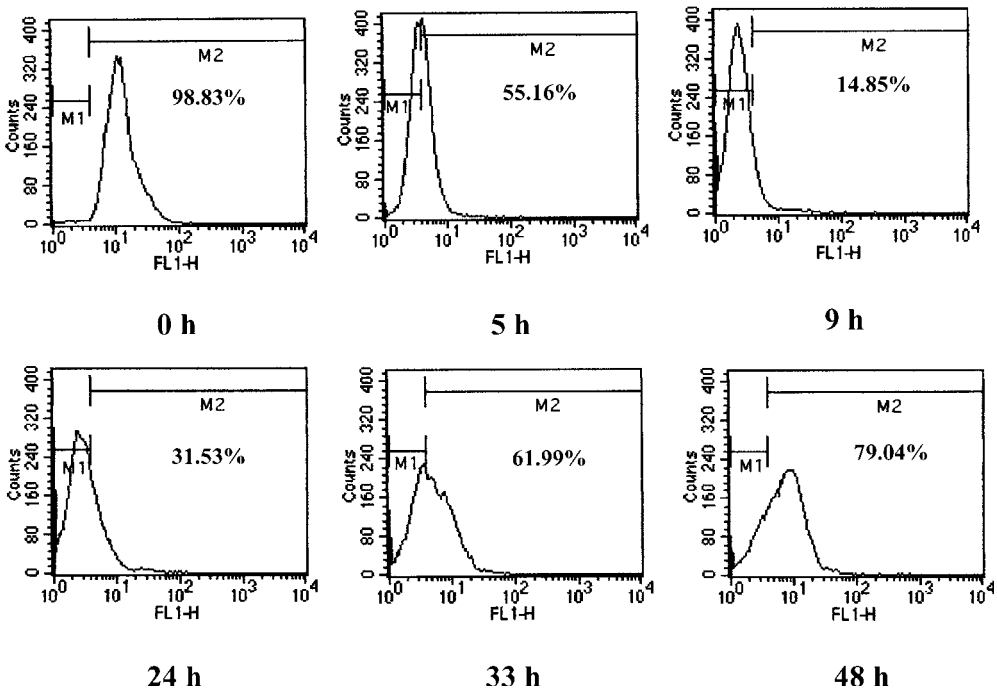

Fig. 7 Effect of diosgenin on cytoplasmic Ca^{2+} concentration in K562 cells. K562 cells were treated with 20 μM diosgenin for the indicated times. Intracellular Ca^{2+} concentrations were determined in terms of the fluorescent activity of Fluo-3 by FACS analysis

Another antiapoptotic protein Bcl-x_L was also down-regulated by diosgenin at 48 h. It is noteworthy that the levels of proapoptotic Bax significantly increased after normalization with reference to β-actin levels (Fig. 10b).

Discussion

Natural products provide one of the most important sources of promising leads for the development of novel chemotherapeutics. The effects on K562 cells of the plant steroid, diosgenin, were investigated in this study. The results clearly demonstrated that diosgenin initiated a series of events leading to cell cycle G_2/M arrest and apoptosis, such as the disruption of intracellular Ca^{2+} homeostasis, mitochondrial dysfunction, ROS generation and caspase activation. Diosgenin-induced mitotic block might be a requisite step for subsequent apoptosis, which was supported by the present observations (Fig. 4a). This phenomenon has been described before as the development of an aberrant mitotic exit into a G_1-like "multinucleate state", which eventually progresses into apoptosis [19]. It is not fully understood how cytotoxic stress causes K562 cells to undergo apoptosis at the G_2/M checkpoint. Our results proved that G_2/M arrest could be mainly controlled by cyclin B1 because the G_2/M arrest was consistent with the suppression of cyclin B1 (Fig. 4), which is the regulatory subunit of cdc2 kinase and is required for mitotic initiation. Innocente et al. have reported that p53 arrests the cell cycle in G_2/M by lowering cyclin B1 levels [16], which challenges our observation because K562 cells are deficient in functional p53 [22].

Based on these results and the fact that diosgenin-induced cell cycle arrest also occurs in p53-positive NB_4 cells, the mitotic-arresting effects of K562 cells should be via a distinct signaling pathway that is not dependent upon p53. However, in NB_4 cells, it is speculated that p53 may play an important role in the blocking process (Fig. 5c). The observed multinucleation phenotype represents additional rounds of DNA replication in the absence of cell division or apoptosis, indicating that wild-type p53 can prevent the damaged G_2/M phase cells progressing into mitosis. Our results also showed a relationship between $p21^{Cip1/Waf1}$ levels and the amount of apoptosis, as diosgenin caused a reduction in $p21^{Cip1/Waf1}$ which was synchronous with a concomitant increase in apoptosis. An alternative postulate is that $p21^{Cip1/Waf1}$, as the universally potent CDK inhibitor, was cleaved in the present study, and this has been proved to be a critical step in converting cells from growth arrest to undergoing apoptosis [34]. Caspase-dependent cleavage of $p21^{Cip1/Waf1}$ during apoptosis has also been reported for a number of stimuli, such as tumor necrosis factor [9] and DNA damage [12, 34].

Ca^{2+} is a ubiquitous intracellular messenger, which mediates multiple signaling cascades that are critical for cell survival and apoptosis. The role of intracellular free Ca^{2+} in cell death is a matter of debate. Elevation in the cytosolic Ca^{2+} concentration can lead to apoptosis, owing to mitochondrial Ca^{2+} uptake and consequent overloading, triggering PTP opening and cytochrome *c* release [7]. However, not all dying cells exhibit an increase in Ca^{2+} prior to final membrane failure, as proved in the present study. Diosgenin-induced a dramatic decline in cytoplasmic Ca^{2+} concentration, indicating its extraordinary role in the process of mitotic apoptosis (Fig. 7). Two hypotheses have been proposed to explain the involvement of Ca^{2+}. The first one is that diosgenin may have a direct or indirect effect on

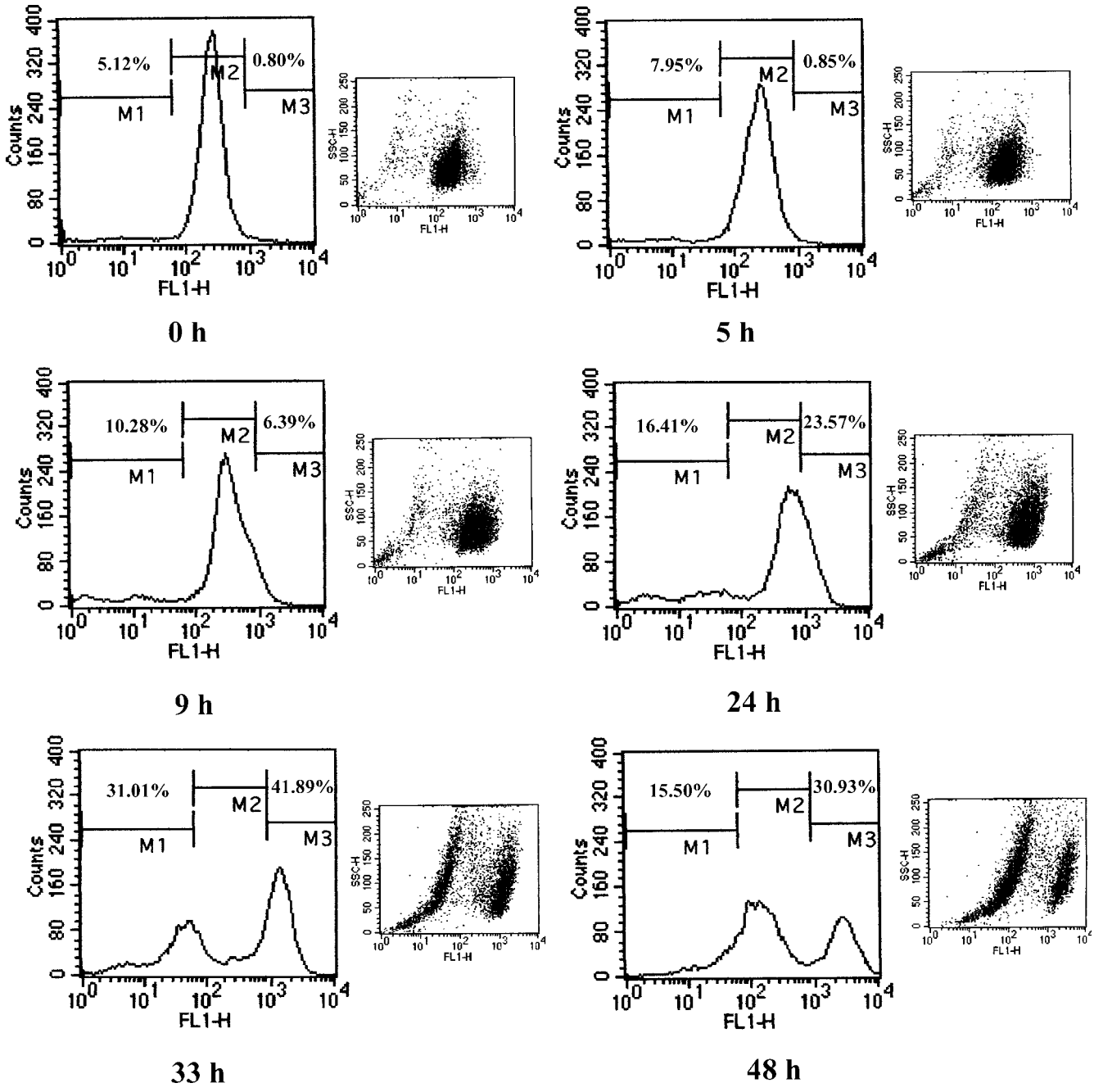

Fig. 8 Time-course analysis of MMP in the process of diosgenin-induced cell cycle arrest and apoptosis. K562 cells were treated with 20 μM diosgenin for the indicated times. The MMP changes were determined in terms of $DiOC_6(3)$ fluorescence by FACS analysis

membrane lipid composition, resulting in the efflux of Ca^{2+} through plasma membrane. The second hypothesis is that the rapid decrease in intracellular Ca^{2+} is predominantly the result of stimulation of the mitochondrial Ca^{2+} uptake. This process requires oxidative phosphorylation and is energy-dependent, which may benefited from the increased $\Delta\Psi_m$, because the uptake process by the uniporter is driven by a negative MMP ($\Delta\Psi_m$) [20]. The maintenance of a normal $\Delta\Psi_m$ is crucial to the homeostasis of intramitochondrial Ca^{2+} levels. Changes in $\Delta\Psi_m$ correlated with fluctuations in cytosolic Ca^{2+} as modulated by plasma membrane and endoplasmic reticulum Ca^{2+} pumps.

Our results establish a close relationship between the alterations of Ca^{2+} homeostasis and the mitochondrial events in affected cells. Fluo-3 fluorescence had dropped below that of the control cells by 5 h after treatment and minimal values were seen at 9 h. During the same period, there was an elevation in $DiOC_6(3)$ fluorescence (Fig. 8). By 33 h, K562 cells showed clear morphological evidence of apoptosis; the fluorescence of $DiOC_6(3)$ had become two peaks while the cytosolic Ca^{2+} concentration was restored. It is tempting to speculate that the initial mitochondrial hyperpolarization was an

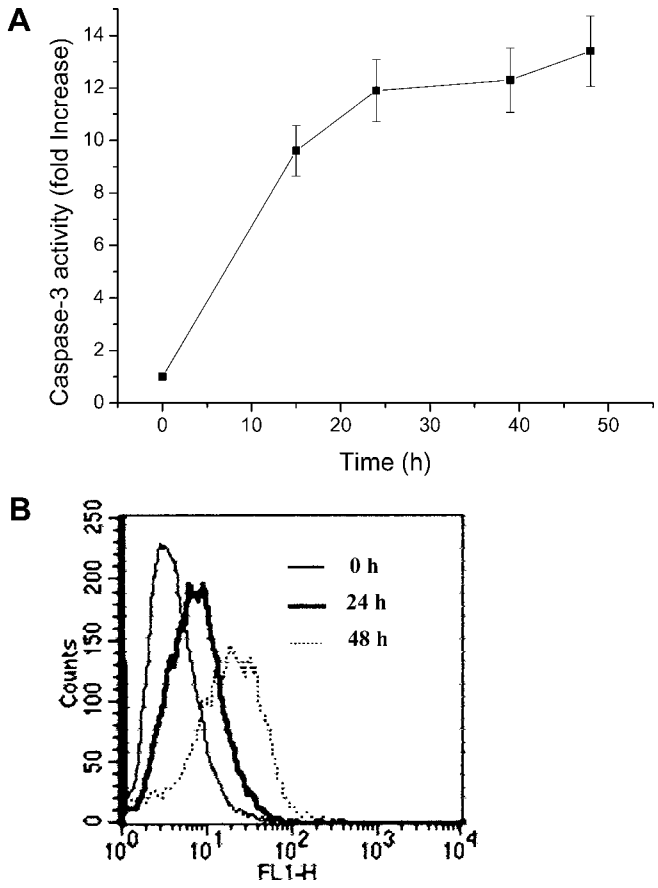

Fig. 9a, b The activation of caspase-3 and the generation ROS were involved in diosgenin-induced apoptosis. **a** K562 cells were treated with 20 μM diosgenin for the indicated times. Each data point is the mean of three replicates; *bars* represent the standard deviation. **b** K562 cells were treated with 20 μM diosgenin for the indicated times. The ROS generation was determined in terms of DCFH-DA fluorescence by FACS analysis

immediate reaction to apoptogens or to Ca^{2+} homeostatic disruption. The later intracellular increase of Ca^{2+} concentration was directly related to the loss in MMP and the subsequent dysfunction of the mitochondria. During the later stage, the cytosolic Ca^{2+} may serve to activate downstream effectors, mainly the apoptosis-related proteases such as Ca^{2+}-dependent endonuclease. Ca^{2+} also seems to trigger increased production of ROS as well as the release of proapoptogenic proteins.

In most eukaryotic cells, MMP ($\Delta\Psi_m$) is generated by the respiratory chain or through ATP-dependent reversal of mitochondrial ATP synthase. Catastrophic loss of MMP due to the opening of mitochondrial PTP is an extremely common occurrence in cells undergoing apoptosis. Prior to the loss of MMP, hyperpolarization of the mitochondrial inner membrane during the early stages of apoptosis has been reported [21, 32], as observed in the present study (Fig. 8). The hyperpolarization effects can result from different actions, such as an increased mitochondrial mass and number per cell or an increase in matrix volume [28]. The latter can lead to swelling and rupture of the mitochondrial outer membrane, followed by a depolarization in $\Delta\Psi_m$. We showed that the initial increase in $\Delta\Psi_m$ in K562 cells is consistent with the arrest of the cells in the G_2/M phase and the subsequent disruption of $\Delta\Psi_m$ is associated with the appearance of the sub-G_1 cell fraction. The mitochondrial hyperpolarization may be attributable to the premitotic cells and the depolarization to the apoptotic cells, as indicated in the dual parametric dot plots combining SSC (side scatter) and $DiOC_6(3)$ fluorescence (FL-1) (Fig. 8). The hyperpolarization may also have been driven by respiration increase, as a result of enhanced oxidative phosphorylation and ATP production. It could also be explained by the same mechanism that leads to cytosolic acidification [23]. Diosgenin may have a deleterious effect on the electron transport chain. The membrane hyperpolarization can hold the electron carriers of the respiratory chain in a much reduced state, which makes ROS more easily released [33]. ROS are known as intracellular second messengers at low concentrations and are able to activate transcription factors, such as NF-κB and AP-1. The burst of ROS in the cytosol might act as a mediator in apoptotic pathways and in turn act on MMP to influence mitochondrial function. Thus, mitochondrial Ca^{2+} accumulation and increased ROS production finally lead to irreversible damage to mitochondria, the opening of the PTP, and the triggering of the cell death program.

The Bcl-2 family members appear to interact to regulate the commitment to survive or die upon challenge with various apoptotic stimuli by controlling the flux of ions and proteins through intracellular membranes [14]. Bcl-2 and Bcl-x_L have been shown to exert their inhibitory effects on apoptosis by blocking the release of cytochrome *c* and the decline in MMP. The downregulation of their levels is in conjunction with impairment of their antiapoptotic role. The multinucleated phenotype observed in our studies is similar to that observed in the cooperation between Bcl-x_L and loss of p53 to overcome a mitotic spindle checkpoint [24]. Bax mainly resides in the cytosol and translocates to mitochondria upon receiving an apoptotic signal, where it may initiate homodimerization or heterodimerization, resulting in mitochondrial dysfunction [14]. The level of proapoptotic Bax was increased in this study when the cells were treated with diosgenin for 36 h (Fig. 10). This contributes the additional observations that Bax membrane insertion is a late event, which occurs subsequent to rather than concomitantly with cell cycle arrest in the G_2/M phase. In addition, Bcl-2 enhances mitochondrial Ca^{2+} loading and enables cells to maintain a stable $\Delta\Psi_m$ [35], whereas Bak and Bax involve direct effects on sensitization of mitochondria to Ca^{2+}-mediated fluxes and cytochrome *c* release [27]. The changes in Bcl-2 and Bax coincided with the restoration of intracellular Ca^{2+}, indicating their role in regulating ion release from mitochondria.

In conclusion, diosgenin caused cell cycle G_2/M arrest and apoptosis in human leukemia K562 cells. The results revealed the associations between Ca^{2+}

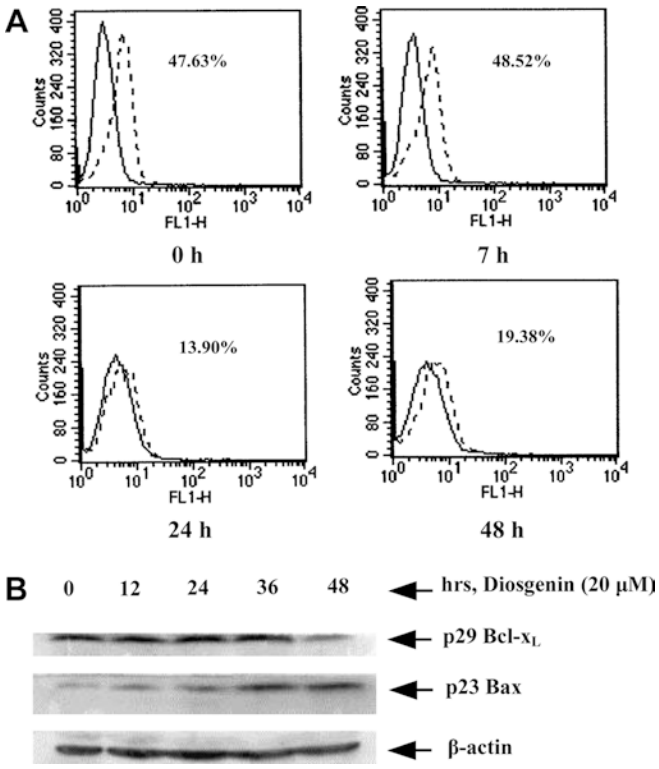

Fig. 10a, b Regulation of Bcl-2 family members by diosgenin. **a** Immunofluorescence analysis of Bcl-2 expression. The *solid lines* indicate mouse $IgG_{1\kappa}$ used as isotype control while the *dotted lines* represent diosgenin-treated K562 cells. At least 10,000 events were counted. The data shown are representative of three separate experiments. **b** Western blot analysis for the expression levels of Bcl-x_L and Bax

homeostatic disruption, mitochondrial dysfunction, ROS production, and caspase activation. Intracellular Ca^{2+} fluctuation is a pivotal event that leads to mitochondrial dysfunction, with hyperpolarization as a remarkable characteristic in the whole process. This study may provide a mechanistic background for the introduction of this new type of promising therapeutic agent in the study of cancer chemotherapy.

Acknowledgements This work was supported in part by grants from the Tsinghua University, Hong Kong Baptist University Joint Institute for Research of Chinese Medicine, and Tsinghua University's 985 Project.

References

1. Aradhana, Rao AR, Kale RK (1992) Diosgenin—a growth stimulator of mammary gland of ovariectomized mouse. Indian J Exp Biol 30:367
2. Arion D, Meijer L, Brizuela L, Beach D (1988) cdc2 is a component of the M phase-specific histone H1 kinase: evidence for identity with MPF. Cell 55:371
3. Attele AS, Wu JA, Yuan CS (1999) Ginseng pharmacology: multiple constituents and multiple actions. Biochem Pharmacol 58:1685
4. Beneytout JL, Nappez C, Leboutet MJ, Malinvaud G (1995) A plant steroid, diosgenin, a new megakaryocytic differentiation inducer of HEL cells. Biochem Biophys Res Commun 207:398
5. Corbiere C, Liagre B, Bianchi A, Bordji K, Dauca M, Netter P, Beneytout JL (2003) Different contribution of apoptosis to the antiproliferative effects of diosgenin and other plant steroids, hecogenin and tigogenin, on human 1547 osteosarcoma cells. Int J Oncol 22:899
6. Cory S, Adams JM (2002) The Bcl-2 family: regulators of the cellular life-or-death switch. Nat Rev Cancer 2:647
7. Crompton M (1999) The mitochondrial permeability transition pore and its role in cell death. Biochem J 34:1233
8. Desagher S, Martinou JC (2000) Mitochondria as the central control point of apoptosis. Trends Cell Biol 10:369
9. Donato NJ, Perez M (1998) Tumor necrosis factor-induced apoptosis stimulates p53 accumulation and $p21^{WAF1}$ proteolysis in ME-180 cells. J Biol Chem 273:5067
10. Duchen MR (1999) Contributions of mitochondria to animal physiology: from homeostatic sensor to calcium signaling and cell death. J Physiol 516:1
11. Elledge SJ (1996) Cell cycle checkpoints: preventing an identity crisis. Science 274:1664
12. Gervais JL, Seth P, Zhang H (1998) Cleavage of CDK inhibitor p21(Cip1/Waf1) by caspases is an early event during DNA damage-induced apoptosis. J Biol Chem 273:19207
13. Green DR, Reed JC (1998) Mitochondria and apoptosis. Science 281:1309
14. Gross A, McDonnell JM, Korsmeyer SJ (1999) BCL-2 family members and the mitochondria in apoptosis. Genes Dev 13:1899
15. Hu K, Dong A, Yao X, Kobayashi H, Iwasaki S (1996) Antineoplastic agents. I. Three spirostanol glycosides from rhizomes of Dioscorea collettii var. hypoglauca. Planta Med 62:573
16. Innocente SA, Abrahamson JL, Cogswell JP, Lee JM (1999) p53 regulates a G_2 checkpoint through cyclin B1. Proc Natl Acad Sci U S A 96:2147
17. Jiang X, Wang X (2000) Cytochrome c promotes caspase-9 activation by inducing nucleotide binding to Apaf-1. J Biol Chem 275:31199
18. Johnstone RW, Ruefli AA, Lowe SW (2002) Apoptosis: a link between cancer genetics and chemotherapy. Cell 108:153
19. Jordan MA, Wendell K, Gardiner S, Derry WB, Copp H, Wilson L (1996) Mitotic block induced in HeLa cells by low concentrations of paclitaxel (Taxol) results in abnormal mitotic exit and apoptotic cell death. Cancer Res 56:816
20. Kroemer G, Dallaporta B, Resche-Rigon M (1998) The mitochondrial death/life regulation of apoptosis and necrosis. Annu Rev Physiol 60:619
21. Li PF, Dietz R, von Harsdorf R (1999) p53 regulates mitochondrial membrane potential through reactive oxygen species and induces cytochrome c independent apoptosis blocked by bcl-2. EMBO J 18:6027
22. Lubbert M, Miller CW, Crawford L, Koeffler HP (1988) p53 in chronic myelogenous leukemia, study of mechanisms of differential expression. J Exp Med 167:873
23. Matsuyama S, Lopis J, Deveraux QL, Tsien RY, Reed JC (2000) Changes in intramitochondrial and cytosolic pH: early events that modulate caspase activation during apoptosis. Nat Cell Biol 2:318
24. Minn AJ, Boise LH, Thompson CB (1996) Expression of bcl-x(L) and loss of p53 can cooperate to overcome a cell cycle checkpoint induced by mitotic spindle damage. Genes Dev 10:12621
25. Moalic S, Liagre B, Corbiere C, Bianchi A, Dauca M, Bordji K, Beneytout JL (2001) A plant steroid, diosgenin, induces apoptosis, cell cycle arrest and COX activity in osteosarcoma cells. FEBS Lett 506:225
26. Nappez C, Liagre B, Beneytout JL (1995) Changes in lipoxygenase activities in human erythroleukemia (HEL) cells during diosgenin-induced differentiation. Cancer Lett 96:133
27. Nutt LK, Pataer A, Pahler J, Fang B, Roth J, McConkey DJ, Swisher SG (2002) Bax and Bak promote apoptosis by modulating endoplasmic reticular and mitochondrial Ca^{2+} stores. J Biol Chem 277:9219

28. Reed JC, Jurgensmeier JM, Matsuyama S (1998) Bcl-2 family proteins and mitochondria. Biochim Biophys Acta 1366:127
29. Roman ID, Thewles A, Coleman R (1995) Fractionation of livers following diosgenin treatment to elevate biliary cholesterol. Biochim Biophys Acta 1255:77
30. Taylor WR, Stark GR (2001) Regulation of the G_2/M transition by p53. Oncogene 20:1803
31. Thornberry NA, Rano TA, Peterson EP, Rasper DM, Timkey T, Garcia-Calvo M, Houtzager VM, Nordstrom PA, Roy S, Vaillancourt JP, Chapman KT, Nicholson DW (1997) A combinatorial approach defines specificities of members of the caspase family and granzyme B. Functional relationships established for key mediators of apoptosis. J Biol Chem 272:17907
32. Vander Heiden MG, Chandel NS, Schumacker PT, Thompson CB (1999) Bcl-x_L prevents cell death following growth factor withdrawal by facilitating mitochondrial ATP/ADP exchange. Mol Cell 3:159
33. Wallace KB, Eells JT, Madeira VMC, Cortopassi G, Jones DP (1997) Mitochondria-mediated cell injury. Fundam Appl Toxicol 38:23
34. Zhang Y, Fujita N, Tsuruo T (1999) Caspase-mediated cleavage of $p21^{Waf1/Cip1}$ converts cancer cells from growth arrest to undergoing apoptosis. Oncogene 18:1131
35. Zhu L, Ling S, Yu XD, Venkatesh LK, Subramanian T, Chinnadurai G, Kuo TH (1999) Modulation of mitochondrial Ca^{2+} homeostasis by Bcl-2. J Biol Chem 274:33267